nature cell biology

Identification of the cell lineage at the origin of basal cell carcinoma

Khalil Kass Youssef[1,3], Alexandra Van Keymeulen[1,3], Gäelle Lapouge[1,3], Benjamin Beck[1], Cindy Michaux[1], Younes Achouri[2], Panagiota A. Sotiropoulou[1] and Cédric Blanpain[1,4]

For most types of cancers, the cell at the origin of tumour initiation is still unknown. Here, we used mouse genetics to identify cells at the origin of basal cell carcinoma (BCC), which is one of the most frequently occurring types of cancer in humans, and can result from the activation of the Hedgehog signalling pathway. Using mice conditionally expressing constitutively active Smoothened mutant (*SmoM2*), we activated Hedgehog signalling in different cellular compartments of the skin epidermis and determined in which compartments Hedgehog activation induces BCC formation. Activation of *SmoM2* in hair follicle bulge stem cells and their transient amplifying progenies did not induce cancer formation, demonstrating that BCC does not originate from bulge stem cells, as previously thought. Using clonal analysis, we found that BCC arises from long-term resident progenitor cells of the interfollicular epidermis and the upper infundibulum. Our studies uncover the cells at the origin of BCC in mice and demonstrate that expression of differentiation markers in tumour cells is not necessarily predictive of the cancer initiating cells.

Stem cells are responsible for the maintenance of adult tissues, a process called homeostasis, and tissue repair following injuries. Stem cells have been hypothesized to be the cells at the origin of cancer as they reside and self-renew in tissues for extended periods of time, increasing their lifetime risk of accumulating the oncogenic mutations required for cancer formation[1,2]. Two epithelial skin cancers occur frequently in human populations: squamous cell carcinoma and BCC[3,4]. BCC is a common human cancer (700,000 new cases are diagnosed each year in US) that arises from sun-exposed parts of the skin epidermis[5]. BCC is a slow growing and locally invasive cancer that is thought to arise from hair follicles[3,4,6]. Loss of heterozygosity of Patched, or activating mutations in Smoothened gene (*SmoM2*) leading to constitutive activation of the Hedgehog (HH) pathway are found in most sporadic or inherited forms of BCC[5,7–9]. Mouse BCC is identical to human skin cancers[10–14] and thus offers an ideal model to identify the cells at the origin of BCC initiation. Skin epidermis is composed of different discrete histologically and biochemically identifiable compartments containing hair follicles, sebaceous glands and their surrounding interfollicular epidermis (Supplementary Information, Fig. S1)[15]. Multipotent stem cells residing in the specialized part of the hair follicle called the bulge are responsible for hair follicle regeneration during homeostasis, but also contribute to interfollicular epidermis repair during wound healing[16–21]. Bulge stem cells represent a reservoir of multipotent stem cells able to differentiate into all epidermal lineages; however, maintenance of the interfollicular epidermis, the infundibulum (the part of the epidermis that connects the hair follicle to the interfollicular epidermis), as well as the isthmus and the sebaceous glands is ensured, independently of bulge stem cells, by the presence of different resident stem cells[22–29].

One of the key unresolved questions in cancer biology is the identification of cells at the origin of cancer. Here, we used a genetic approach to identify cells at the origin of BCC in mice (Supplementary Information, Fig. S1). To ensure that every targeted tissue compartment received intrinsically the same dose of activated HH signalling, we used mice that conditionally expressed *SmoM2* oncogene under the control of the ubiquitously expressed *ROSA26* promoter, and which recapitulate all cancers resulting from constitutive HH pathway activation, including BCC[13,30]. We first induced *SmoM2* expression in most of the epidermal cells by administering a high dose of tamoxifen (15 mg total) to K14-CREER/*RosaSmoM2* mice aged 28 days (D28; Fig. 1a), which results in constitutive HH activation in basal proliferative cells and progressively in their differentiated progenies, encompassing every cellular compartment of the skin epidermis[31]. In the absence of tamoxifen, no expression of *SmoM2* was detectable, demonstrating the absence of leakiness (Fig. 1b), whereas administration of tamoxifen (15 mg) over 5 days induced *SmoM2* expression in most of the epidermal cells (Fig. 1c). Immunofluorescence microscopy and FACS analysis showed that *Rosa26* promoter-induced expression is similar in the different epidermal compartments (Fig. 1d; Supplementary Information, Fig. S2). Macroscopically visible BCC began to be detectable 8 weeks after tamoxifen administration, preferentially in the tail and ear regions (Fig. 1e, h), as previously reported in other BCC mouse models[6]. Microscopically, these BCC

[1]Université Libre de Bruxelles (ULB), IRIBHM, Brussels B-1070, Belgium. [2]Université catholique de Louvain, de Duve Institute, Brussels B-1200, Belgium.
[3]These authors contributed equally to the work.
[4]Correspondence should be addressed to: C.B. (e-mail: Cedric.Blanpain@ulb.ac.be)

Received 23 October 2009; accepted 25 January 2010; published online 14 February 2010; DOI: 10.1038/ncb2031

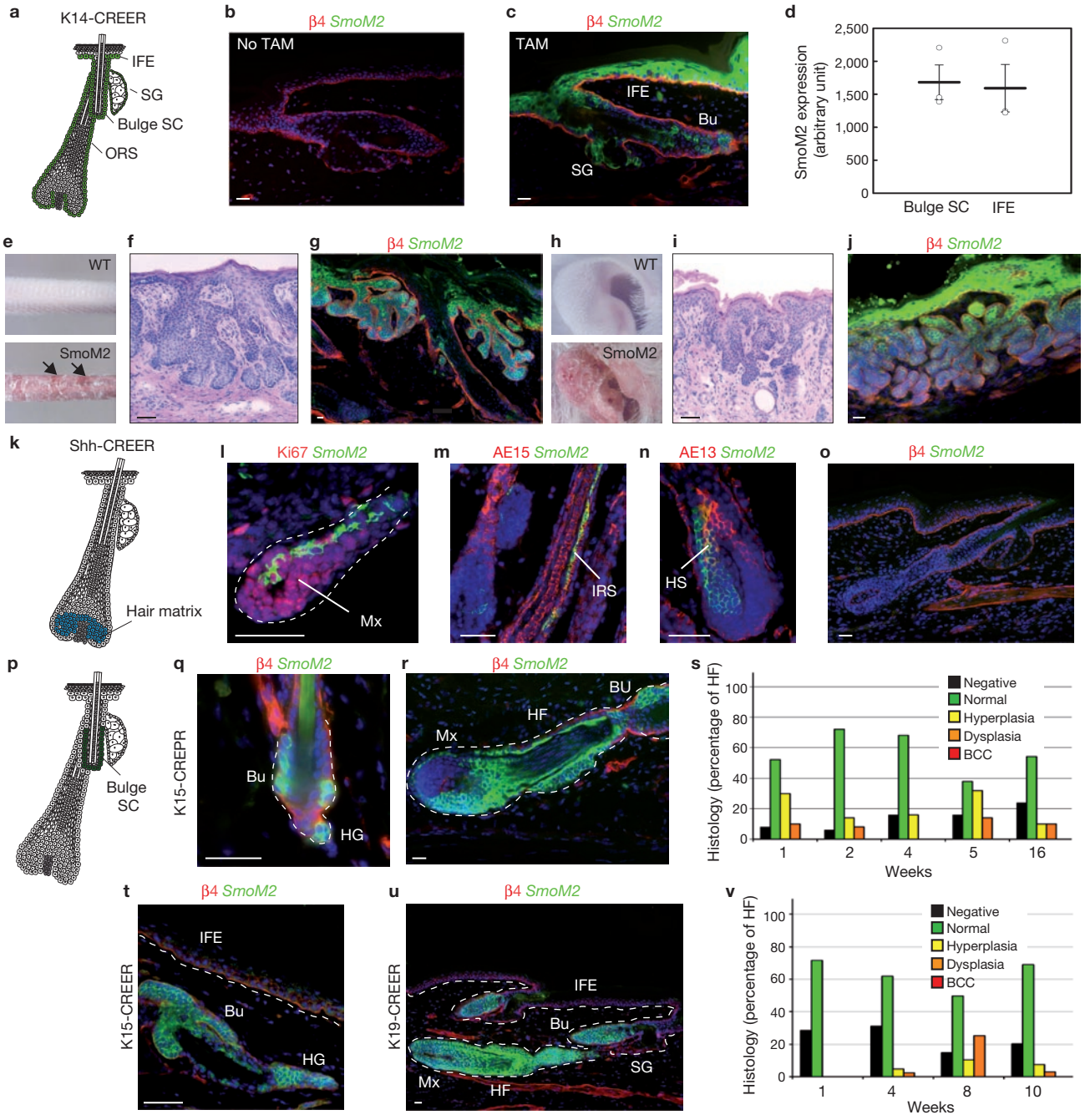

Figure 1 BCCs do not arise from hair follicle bulge stem cells and their progenies. (**a**) Epidermal cells targeted by the K14 promoter, highlighted in light green. (**b**) No leakiness in the absence of tamoxifen (TAM). (**c**) *SmoM2* expression 1 week after TAM (15 mg) administration. (**d**) FACS analysis of *SmoM2* expression in bulge stem cells (α6+CD34H) and in the interfollicular epidermis (α6HCD34–) 1 week after TAM administration. Data are mean ± s.e.m ($n = 3$ mice). (**e–j**) BCC in tail (**e–g**) and ear (**h–j**) of K14–CREER/*RosaSmoM2* mice 10 weeks after TAM (15 mg) administration. Macroscopic pictures of mouse tail (**e**) and ear (**h**). (**f, i**) Haematoxylin–eosin staining of tail (**f**) and and ear (**i**). (**g, j**) Immunofluorescence staining showing *SmoM2* expressing cells in tail (g) and ear (j). (**k–o**) *SmoM2* expression in hair follicle transit amplifying cells using Shh-CREER/*RosaSmoM2* does not lead to cancer formation. Matrix cells targeted by the Shh promoter (**k**) are highlighted in light blue. Immunofluorescence of cells expressing *RosaSmoM2* cells with a marker of cell proliferation (Ki67) (**l**), and markers of the inner root sheath (AE15) (**m**) and the hair shaft (AE13) differentiation (**n**) 1 week after TAM administration. No SmoM2 expressing cells or BCC were observed 10 weeks following SmoM2 expression (**o**). (**p**) Bulge stem cells targeted by the K15 and K19 promoters are highlighted in dark green. (**q, r**) *SmoM2* activation in hair follicle of K15-CREPR/*RosaSmoM2* mice 1 day after RU486 (7.5 mg) induction (**q**) and 10 weeks after *SmoM2* expression (**r**). (**s**) Quantification of the histology of *SmoM2*-expressing hair follicle in K15-CREPR/*RosaSmoM2* mice, showing that *SmoM2* expression in hair follicle can induce dysplastic lesions but does not lead to BCC development. Data are mean ± s.e.m ($n = 50$ follicular units per time point from 2 different mice) (**t**) *SmoM2* expression in hair follicles 10 weeks after TAM (8 mg) induction in K15-CREER/*RosaSmoM2* mice. (**u**) *SmoM2* expression in hair follicle 10 weeks after TAM (10 mg) induction in K19-CREER/*RosaSmoM2* mice. (**v**) Quantification of the histology of *SmoM2* expressing hair follicles in K19-CREER/*RosaSmoM2* mice. Data are mean ± s.e.m ($n = 205, 126, 443, 265$ follicular units analysed at 1, 4, 8, and 10 weeks respectively from two different mice). Scale bars, 50 μm (Bu, bulge; IFE, interfollicular epidermis; SG, sebaceous gland; HG, hair germ; Mx, matrix; IRS, inner root sheath; HS, hair shaft).

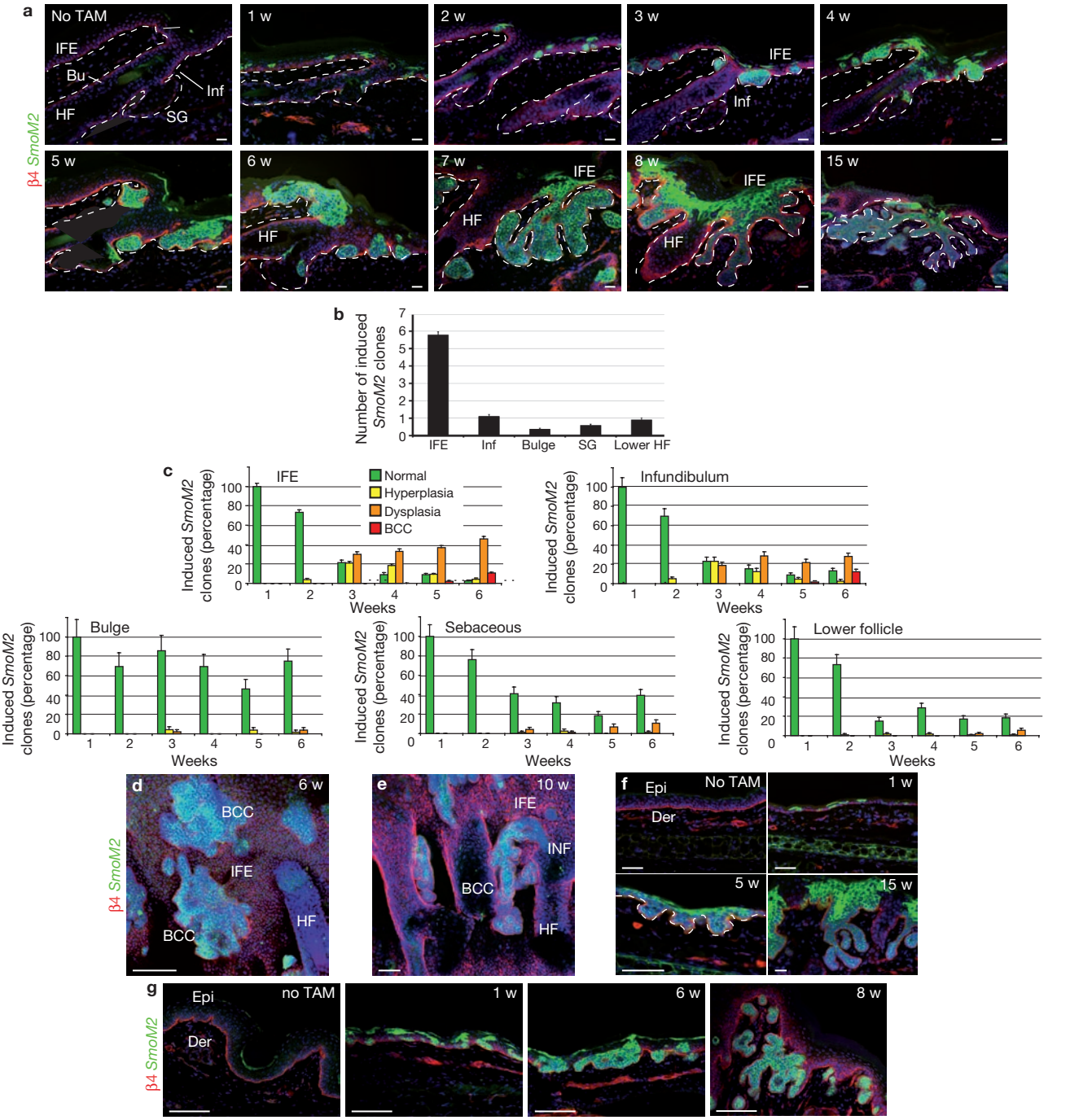

Figure 2 BCC originates from cells residing in the interfollicular epidermis and the infundibulum. (**a**) Histological evolution of *SmoM2* expressing clones in tail epidermis in K14-CREER/*RosaSmoM2* mice from 1–15 weeks after tamoxifen (1 mg, TAM) administration. (**b**) Average number of *SmoM2* clones induced in each epidermal compartment. Data are mean ± s.e.m (n =108 interfollicular and follicular units from two different mice) (**c**) Quantification of the percentage of induced clones presenting a normal, hyperplastic, dysplastic or BCC histology over time in the different epidermal compartments in K14-CREER/*RosaSmoM2* mice. Data are mean ± s.e.m (n = 108, 108, 126, 124, 150 and 183 interfollicular and follicular units analysed from two different mice at 1, 2, 3, 4, 5 and 6 weeks, respectively, which correspond to 942, 716, 713, 570, 637, and 733 *SmoM2* clones analysed at these different time-points). BCC only occurs in interfollicular epidermis and infundibulum compartments. (**d**, **e**) Confocal analysis of whole-mount tail epidermis following *SmoM2* expression showing that BCC arise from the interfollicular epidermis (**d**) and the upper infundibulum (**e**). (**f**) *SmoM2*-expressing clones in ear epidermis 1, 5 and 15 weeks after TAM (1 mg) administration. (**g**) BCC arising from hairless paw epidermis in K14-CREER/*RosaSmoM2* mice 8 weeks after TAM administration. Scale bars, 50 μm. (Bu, bulge; IFE, interfollicular epidermis; SG, sebaceous gland; inf, infundibulum).

lesions presented all the histological features of human nodular BCC[32], invading the underlying dermis with a typical appearance of branched basal hair follicle like structure (Fig. 1f–j).

To determine whether *SmoM2* activation in hair follicle transit amplifying progenitors can induce BCC formation, we induced *SmoM2* activation in hair follicle matrix cells using Shh-CREER mice[33] (Fig. 1k).

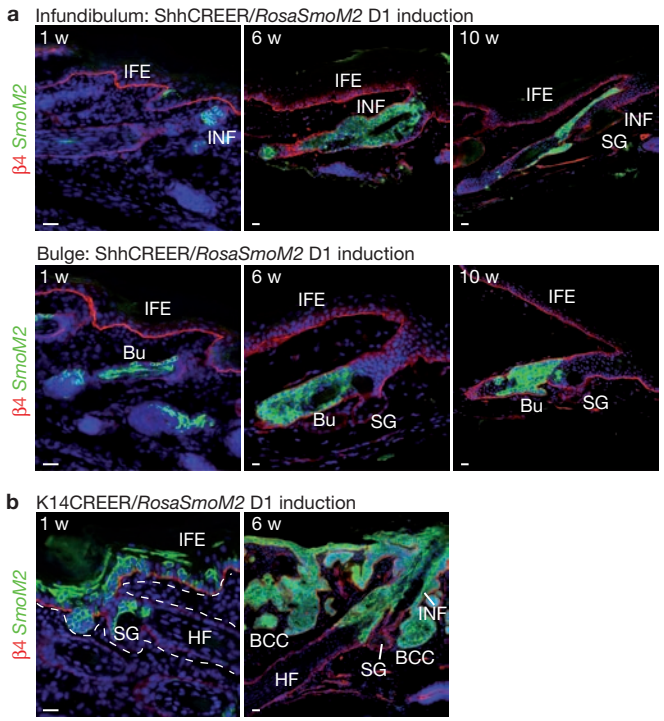

Figure 3 BCC does not arise from Shh-derived hair follicle and infundibulum cells. (**a**) Immunostaining of Shh-CREER/*RosaSmoM2* mice induced with tamoxifen (0.2 mg) at birth (D1) shows the labelling of cells in the prospective infundibulum (upper panels) and bulge (lower panels) 1 week after induction. No BCC was observed 6 or 10 weeks after *SmoM2* expression in these two epidermal compartments. (**b**) Dysplasia and BCC were observed after tamoxifen administration in K14-CREER/*RosaSmoM2* mice at 1 and 6 weeks, respectively, showing that the absence of BCC formation in Shh-CREER is not the result of incompetence of the epidermis to form BCC at this age. Scale bars, 50 μm (IFE, Interfollicular epidermis; Bu, Bulge; SG, sebaceous gland; inf, infundibulum).

During hair follicle regeneration, transit amplifying matrix cells reside at the base of the hair follicle and express high levels of Shh[34]. After tamoxifen administration in Shh–CREER mice, *SmoM2* expression was observed in matrix progenitor cells (Fig. 1l) and their hair follicle progenies, without affecting their terminal differentiation program (Fig. 1m–n). The permanent oncogene expression in transit amplifying matrix cells did not extend the renewal abilities of these cells, and after several rounds of cell division, *SmoM2*-expressing matrix cells stopped proliferating and differentiated into various hair follicle lineages (Fig. 1m–n). BCC has never been observed, macroscopically or microscopically, in mice in which *SmoM2* has been induced in transit amplifying matrix cells using Shh-CREER up to 10 weeks (Fig. 1o). These results demonstrate that *SmoM2* activation is not able to re-induce and extend the long-term self-renewal potential of matrix progenitors, and these cells do not contribute to BCC initiation.

To determine whether the long-term self-renewing property of multipotent bulge stem cells can influence the initiation of BCC, we induced activation of *SmoM2* in bulge stem cells using three different types of inducible CRE (K15-CREPR, K15-CREER and K19-CREER) expressed in the bulge stem cells and their hair follicle progenies[19,35] (Fig. 1p). Labelling of the bulge and hair follicle progenies after tamoxifen administration in *RosaYFP*/K15-CREER and K19–CREER were identical to the previous lineage tracing reports using K15-CREPR (Supplementary Information, Fig. S3), showing that bulge stem cells contribute to hair follicle regeneration, and that there is no contribution of bulge stem cells to the maintenance of interfollicular epidermis or infundibulum during adult homeostasis[18–20]. Administration of CRE-inducible drug during telogen to anagen transition (D21 to D28) in bulge-expressing inducible CRE/*RosaSmoM2* mice resulted in *SmoM2* expression in bulge stem cells (Fig. 1q) and subsequently in their hair follicle progenies (Fig. 1r). Despite the continuous *SmoM2* expression, hair follicles continued to undergo their physiological cycle of growth and degeneration (Supplementary Information, Fig. S4), suggesting that constitutive HH signalling does not lead to continuous activation of multipotent bulge stem cells.

Despite the persistence of *SmoM2* expression in bulge stem cell and their hair follicle progenies for months, only rare *SmoM2*-targeted hair follicle cells became hyperplastic or dysplastic, and these mice did not develop any sign of BCC formation originating from bulge stem cells and their progenies even 16 weeks after oncogene activation (Fig. 1r–v; Supplementary Information, Fig. S5a–c), a time-point after which many BCC are macroscopically and microscopically visible in K14-CREER mice (Fig.1 e–j). RT–PCR analysis and immunostaining analysis showed that *Gli1*, *Gli2*, *Ptch1* and *Ptch2*, all well-characterized HH target genes, were upregulated after *SmoM2* expression in bulge stem cell and interfollicular epidermis basal cells (Supplementary Information, Fig. S6), demonstrating that the absence of BCC after *SmoM2* expression in hair follicle cells did not result from the inability of bulge stem cells and their progenies to respond to *SmoM2* expression.

To identify which cells of the epidermis must be targeted to induce BCC formation, we performed clonal analysis during BCC development. By administering a low dose of tamoxifen (1 mg) in K14-CREER/*RosaSmoM2*, we induced expression of about 10 positive cells per unit of tail epidermis in the interfollicular epidermis, infundibulum, bulge stem cell, sebaceous glands and lower hair follicle (below the bulge), which were sufficiently distant to unambiguously follow the evolution of each independent clone until BCC development (Fig. 2a). Temporal analysis after oncogene induction revealed that *SmoM2*-targeted cells adopt different fates during clonal evolution that can be easily identified histologically: some clones maintained normal histology and differentiation programs, some clones became hyperplastic but retained a normal shape, whereas other clones persisted as dysplastic lesions presenting placode-like morphology, and finally, some clones degenerated into BCC, with their typical histological appearance of highly branched and undifferentiated cellular downgrowths invading the dermis (Fig. 2a–c; Supplementary Information, Fig. S5d–g). For the first two weeks after *SmoM2* expression, the histology of *SmoM2*-expressing clones was normal. However, after 3 weeks, the proportion of dysplastic clones rapidly increased with time and at 5 weeks some clones located in the interfollicular epidermis and in the upper infundibulum had degenerated into BCC (Fig. 2c). The same frequency of interfollicular epidermis and the upper infundibulum targeted clones progressed to dysplastic and BCC lesions 6 weeks after *SmoM2* expression, suggesting that interfollicular epidermis and infundibulum cells are similarly competent in inducing BCC formation. However, the much higher number of *SmoM2* cells (5-fold) in the interfollicular epidermis presenting such competence explains why BCC arise mostly from the interfollicular epidermis (Fig. 2b, c). As the clones enlarged in size with time, it was difficult to precisely determine using two-dimensional analysis of skin sections whether some BCC originate from the interfollicular epidermis close to its contact with the hair follicle

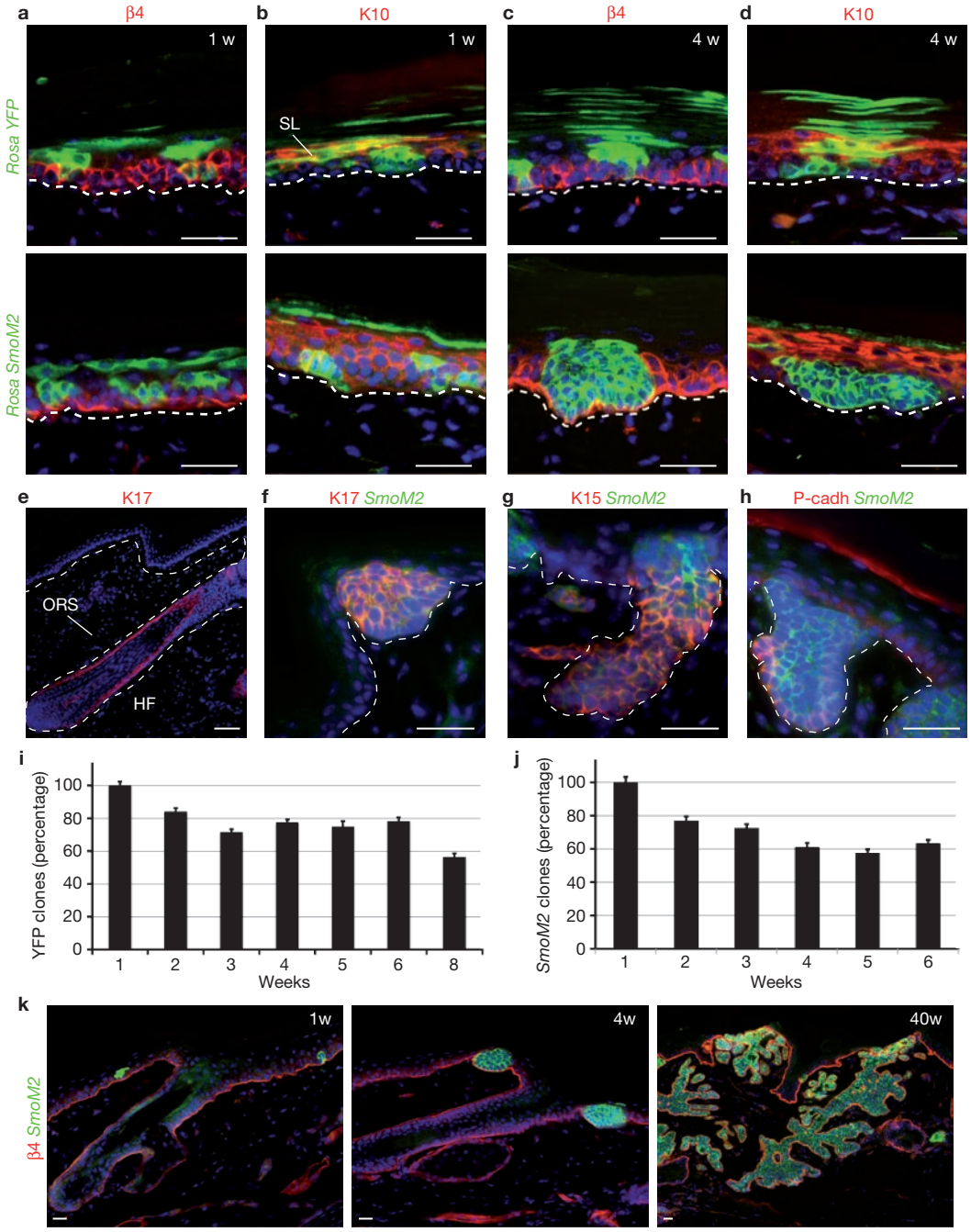

Figure 4 BCC originates from long-lived resident progenitor cells of the interfollicular epidermis. (**a**–**d**) Comparison between K14-CREER/*RosaYFP* (upper panel) and K14-CREER/*RosaSmoM2* (lower panel) clones. Co-staining with β4 integrin (**a**, **c**) or K10 (**b**, **d**) 1 week (**a**, **b**) or 4 weeks (**c**, **d**) after tamoxifen (1 mg) administration. (**e**–**h**) Expression of hair follicle markers in wild-type (**e**) and *SmoM2*-expressing interfollicular epidermis dysplasia (**f**–**h**). K17 (**e**, **f**), K15 (**g**) and P-cadh (**h**). (**i**, **j**) Quantification of the persistence of induced basal clones in the interfollicular epidermis in K14-CREER/*RosaYFP* (**i**) and K14-CREER/*RosaSmoM2* mice over time (**j**), showing a similar percentage of remaining clones after *YFP* or *SmoM2* expression. Data are mean ± s.e.m (n = 188, 142, 174, 133, 57, 120 and 146 interfollicular units analysed from two different mice at 1, 2, 3, 4, 5, 6 and 8 weeks, respectively, which correspond to 801, 509, 531, 439, 182, 399 and 351 YFP clones analysed at these different time-points) (**k**) Long-term clonal analysis in K14-CREER/*RosaSmoM2* mice after a very low dose of tamoxifen (0.2 mg) shows that all long-term *SmoM2*-targeted clones eventually progressed into BCC. Scale bars, 50 μm (BL, basal layer, SL, spinous layer).

or from the upper part of the infundibulum. To unambiguously determine from which cells BCC arise, we performed confocal microscopy analysis of whole mount tail epidermis 6 and 10 weeks after oncogene expression. This three-dimensional analysis of 171 BCCs revealed that 93% of the BCC indeed originated from interfollicular epidermis, whereas the remaining BCC originated from the infundibulum (Fig. 2d, e). The size of BCCs originating from the infundibulum was also smaller than that from the interfollicular epidermis (Fig. 2e). In addition, targeting *SmoM2* in basal cells of the ear interfollicular epidermis, which contains much fewer hair follicles (Fig. 2f), and in the paw epidermis (Fig. 2g),

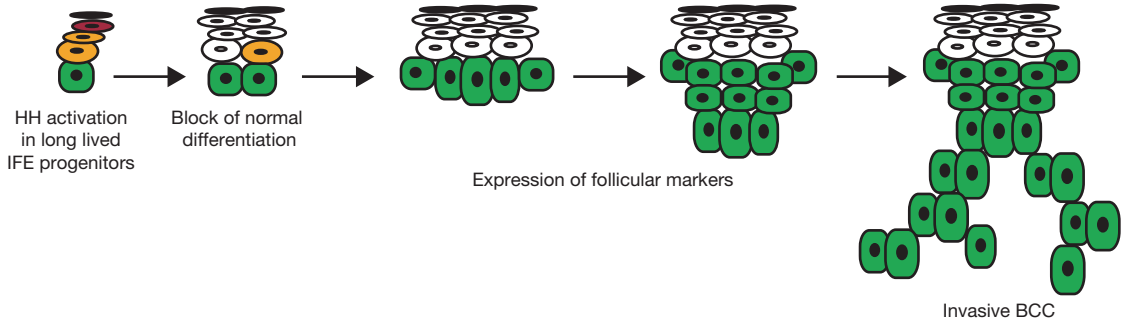

Figure 5 Model of BCC initiation in adult mice. Hedgehog (HH) activation in interfollicular long-lived progenitors induces a block of their normal differentiation and induces expression of hair follicle markers before progression into invasive BCC.

which does not contain hair follicles, also led to BCC transformation with similar kinetics of occurrence to the BCC originating from the tail epidermis, reinforcing the view that BCC originate mostly from cells of the interfollicular epidermis.

Since about half of the infundibulum cells present the same embryonic origin as hair follicle bulge stem cells as demonstrated by Shh–CRE lineage tracing during morphogenesis[20], we determined whether infundibulum cells originating from Shh-expressing cells were also competent to give rise to BCC. Administration of tamoxifen to ShhCREER/*RosaSmoM2* mice at postnatal D1 resulted in *SmoM2* expression in infundibulum cells, as well as in cells of the lower hair follicle (Fig. 3a), as observed in Shh–CRE mice[20]. *SmoM2* expression in Shh-derived infundibulum cells did not induce BCC formation even after 10 weeks of oncogene expression (Fig. 3a). By contrast, tamoxifen administration in K14CREER/*RosaSmoM2* mice at the same age resulted in the development of many BCCs, including in cells of the infundibulum, which completely covered the epidermis only 6 weeks after *SmoM2* expression (Fig. 3b), suggesting that the embryonic origin of infundibulum cells is important in controlling their competence to form BCC. However, our study does not rule out the possibility that the microenvironment may also influence BCC initiation, as regional differences between the different epidermal compartments may be regulated in part by extrinsic factors. In addition, if a group of basal cells collectively progress to BCC, their influence on the stroma microenvironment to promote BCC progression may be critically dependent on the size, density and geometry of the oncogene targeted cells as well. The embryonic origin of the rest of the infundibulum cells that are not targeted by Shh–CRE during morphogenesis remains unclear. One possibility would be that these cells are not targeted by the CRE because of the transient expression of Shh during hair follicle morphogenesis. Alternatively, these cells may arise from isthmus progenitors, which have been identified recently[25,26,29]. However, in the absence of lineage tracing of isthmus progenitors or promoters that specifically target isthmus progenitors, we could not directly determine the competence of these putative infundibulum progenitors during BCC initiation.

Homeostasis of the interfollicular epidermis is ensured by the presence of unipotent progenitors residing along the basal layer of the interfollicular epidermis[15]. Although no specific marker for interfollicular epidermis progenitors has been identified so far, lineage tracing and clonal analysis experiments in mice and human grafted cells have been used to mark the long-term resident progenitors of the interfollicular epidermis and have shown that the interfollicular epidermis is organized into several small epidermal proliferative units (EPU) consisting of several basal cells including progenitors, which differentiate vertically as a column of stacked cells[23,24,28]. Previously, the EPUs were thought to be composed of basal interfollicular epidermis stem cells and transit amplifying cells, as well as suprabasal differentiated cells[36]. However, more recent lineage tracing experiments have shown that, although the interfollicular epidermis is maintained by long-lived progenitor cells, the EPUs do not present the geometry and the size expected from the classical hexagonal model[28,37]. Through mathematical modelling, Jones and colleagues suggested that homeostasis of the epidermis could be maintained by one unique long-lived progenitor rather than stem cell and transit amplying cells, and the rate of epidermal homeostasis is influenced by the rate of cell proliferation and the probability of progenitor differentiation[28]. To determine whether long-lived progenitors of the interfollicular epidermis are responsible for BCC development on *SmoM2* expression, we quantified the number and the fate of interfollicular epidermis-targeted basal cells in K14CREER/*RosaSmoM2* and K14-CREER/*RosaYFP* mice. Administration of tamoxifen (1mg) induced a comparable number of YFP-marked clones along the interfollicular epidermis separating two hair follicles in K14-CREER/*RosaYFP* (4.5 cells/interfollicular epidermis) and K14-CREER/*RosaSmoM2* (5.8 cells/interfollicular epidermis). During the first three weeks after induction, the YFP-expressing basal cells either progressively differentiated, moved suprabasally, showed normal expression of differentiation markers, and were progressively lost, or were maintained as vertical columns of marked cells expanding from the basal layer to the more differentiated suprabasal layers (Fig. 4a–d). Four weeks after induction, the remaining YFP control clones were seen as columns of marked cells expanding from the basal to the top cornified layer, and their frequency remained relatively stable for up to 8 weeks after induction, consistent with the targeting of resident interfollicular epidermis progenitors (Fig. 4e). *SmoM2*-expressing cells progressively stopped differentiating and were maintained as dysplastic lesions consisting of groups of basal cells adopting a placode-like shape, which do not differentiate upward anymore (Fig. 4c, d). The progressive block of differentiation observed in interfollicular epidermis *SmoM2*-targeted clones coincides with expression of follicular progenitor markers such as K17, K15 and P-cadherin (Fig. 4e–h), potentially explaining why it was previously thought that BCC arises from hair follicle bulge stem cells[3,4]. The similar decrease in the frequency of *SmoM2* and control YFP-targeted clones over time (Fig. 4i, j) suggests that constitutive HH signalling should target long-lived resident progenitors to induce BCC formation. Indeed, if expression of *SmoM2* re-induced long-term renewing potential in otherwise pre-committed or differentiated cells, or if *SmoM2* changed the

probability of resident interfollicular epidermis progenitors to undergo self-renewal or differentiation, we should observe the persistence of a higher percentage of basal *SmoM2* clones, compared with basal YFP clones over time. However, we found a similar decrease in the percentage of basal *SmoM2* and YFP clones over time, consistent with the hypothesis that *SmoM2* does not induce renewing potential in otherwise more committed cells, and *SmoM2* needs to target long-lived interfollicular epidermis progenitors to induce BCC development. To determine the frequency of BCC progression in long-term *SmoM2*-targeted cells, we used a lower dose of tamoxifen (0.2 mg) to induce a lower clonal density, allowing the fate of much larger *SmoM2*-expressing clones to be distinguished, which was not possible after 6 weeks when using tamoxifen at the higher dose (1mg). Using this low clonal density, we found that most, if not all, long-term *SmoM2*- expressing clones eventually progressed into invasive BCC (Fig. 4k), suggesting that cancer progression following *SmoM2* expression in long-lived interfollicular epidermis progenitors is a determining process that does not require rare additional genetic and/or epigenetic events.

The demonstration that in mice BCC originates most frequently from long-lived progenitor cells residing in the interfollicular epidermis (Fig. 5), and not from hair follicle bulge stem cells, as previously thought, is likely to be relevant in humans, as mouse models of BCC recapitulate many key features of human BCC, including the types of mutated oncogenes, their histological and biochemical features, their emergence from murine tail epidermis, which resembles human epidermis more than the murine backskin epidermis, as well as their slow growing characteristic. Also, UV light, one of the main risk factor of BCC in human, has limited penetration in tissue and is much more likely to induce DNA damage in interfollicular epidermis cells than in hair follicle bulge stem cells, which are located deeper in the skin[38]. This finding could be important for other cancers as well, as it clearly demonstrates that the biochemical and morphological characterizations of tumour cells can be misleading in identifying the cells at the origin of cancer. □

METHODS

Methods and any associated references are available in the online version of the paper at http://www.nature.com/naturecellbiology/

Note: Supplementary Information is available on the Nature Cell Biology website.

ACKNOWLEDGMENTS

We thank our colleagues who provided reagents, and whose gifts are cited in the text. We thank C. Govaerts, H. Nguyen, P. Vanderhaeghen and G. Vassart for their critical comments on the manuscript. C.B. and A.V.K. are Chercheur Qualifie of the FRS/FNRS; K.K.Y is a Research Fellow of the FRIA; and G.L. is Collaborateur Scientifique of the FRS/FNRS. This work was supported by a Mandat D'impulsion Scientifique of the FNRS, a career development award of the Human Frontier Science Program Organization, a research grant of the Schlumberger Foundation, the programme CIBLES of the Wallonia Region, the EMBO Young Investigator program and from a starting grant of the European Research Council.

AUTHOR CONTRIBUTION

C.B., K.K.Y., A.V.K., G.L. designed the experiments and performed the data analysis; K.K.Y., A.V.K. and G.L. performed most of the experiments; B.B. and P.S. performed the FACS analysis; C.M. provided technical support; Y.A. generated the new transgenic mice; C.B. wrote the manuscript.

COMPETING FINANCIAL INTERESTS

The authors declare no competing financial interests.

Published online at http://www.nature.com/naturecellbiology
Reprints and permissions information is available online at http://npg.nature.com/reprintsandpermissions

1. Pardal, R., Clarke, M. F. & Morrison, S. J. Applying the principles of stem-cell biology to cancer. *Nature Rev. Cancer* **3,** 895–902 (2003).
2. Clarke, M. F. & Fuller, M. Stem cells and cancer: two faces of Eve. *Cell* **124,** 1111–1115 (2006).
3. Owens, D. M. & Watt, F. M. Contribution of stem cells and differentiated cells to epidermal tumours. *Nature Rev. Cancer* **3,** 444–451 (2003).
4. Perez-Losada, J. & Balmain, A. Stem-cell hierarchy in skin cancer. *Nature Rev. Cancer* **3,** 434–443 (2003).
5. Epstein, E. H. Basal cell carcinomas: attack of the hedgehog. *Nature Rev. Cancer* **8,** 743–754 (2008).
6. Pasca di Magliano, M. & Hebrok, M. Hedgehog signalling in cancer formation and maintenance. *Nature Rev. Cancer* **3,** 903–911 (2003).
7. Johnson, R. L. *et al.* Human homolog of patched, a candidate gene for the basal cell nevus syndrome. *Science* **272,** 1668–1671 (1996).
8. Hahn, H. *et al.* Mutations of the human homolog of Drosophila patched in the nevoid basal cell carcinoma syndrome. *Cell* **85,** 841–851 (1996).
9. Xie, J. *et al.* Activating Smoothened mutations in sporadic basal-cell carcinoma. *Nature* **391,** 90–92 (1998).
10. Grachtchouk, M. *et al.* Basal cell carcinomas in mice overexpressing Gli2 in skin. *Nature Genet.* **24,** 216–217 (2000).
11. Grachtchouk, V. *et al.* The magnitude of hedgehog signaling activity defines skin tumor phenotype. *EMBO J.* **22,** 2741–2751 (2003).
12. Dahmane, N., Lee, J., Robins, P., Heller, P. & Ruiz i Altaba, A. Activation of the transcription factor Gli1 and the Sonic hedgehog signalling pathway in skin tumours. *Nature* **389,** 876–881 (1997).
13. Mao, J. *et al.* A novel somatic mouse model to survey tumorigenic potential applied to the Hedgehog pathway. *Cancer Res.* **66,** 10171–10178 (2006).
14. Fan, H., Oro, A. E., Scott, M. P. & Khavari, P. A. Induction of basal cell carcinoma features in transgenic human skin expressing Sonic Hedgehog. *Nature Med.* **3,** 788–792 (1997).
15. Blanpain, C. & Fuchs, E. Epidermal homeostasis: a balancing act of stem cells in the skin. *Natutre Rev. Mol. Cell Biol.* **10,** 207–217 (2009).
16. Tumbar, T. *et al.* Defining the epithelial stem cell niche in skin. *Science* **303,** 359–363 (2004).
17. Blanpain, C., Lowry, W. E., Geoghegan, A., Polak, L. & Fuchs, E. Self-renewal, multipotency, and the existence of two cell populations within an epithelial stem cell niche. *Cell* **118,** 635–648 (2004).
18. Ito, M. *et al.* Stem cells in the hair follicle bulge contribute to wound repair but not to homeostasis of the epidermis. *Nature Med.* **11,** 1351–1354 (2005).
19. Morris, R. J. *et al.* Capturing and profiling adult hair follicle stem cells. *Nature Biotechnol.* **22,** 411–417 (2004).
20. Levy, V., Lindon, C., Harfe, B. D. & Morgan, B. A. Distinct stem cell populations regenerate the follicle and interfollicular epidermis. *Dev. Cell* **9,** 855–861 (2005).
21. Levy, V., Lindon, C., Zheng, Y., Harfe, B. D. & Morgan, B. A. Epidermal stem cells arise from the hair follicle after wounding. *FASEB J.* **21,** 1358–1366 (2007).
22. Kolodka, T. M., Garlick, J. A. & Taichman, L. B. Evidence for keratinocyte stem cells *in vitro*: long term engraftment and persistence of transgene expression from retrovirus-transduced keratinocytes. *Proc. Natl Acad. Sci. USA* **95,** 4356–4361 (1998).
23. Ghazizadeh, S. & Taichman, L. B. Multiple classes of stem cells in cutaneous epithelium: a lineage analysis of adult mouse skin. *EMBO J.* **20,** 1215–1222 (2001).
24. Ro, S. & Rannala, B. A stop-EGFP transgenic mouse to detect clonal cell lineages generated by mutation. *EMBO Rep.* **5,** 914–920 (2004).
25. Nijhof, J. G. *et al.* The cell-surface marker MTS24 identifies a novel population of follicular keratinocytes with characteristics of progenitor cells. *Development* **133,** 3027–3037 (2006).
26. Jensen, U. B. *et al.* A distinct population of clonogenic and multipotent murine follicular keratinocytes residing in the upper isthmus. *J. Cell Sci.* **121,** 609–617 (2008).
27. Horsley, V. *et al.* Blimp1 defines a progenitor population that governs cellular input to the sebaceous gland. *Cell* **126,** 597–609 (2006).
28. Clayton, E. *et al.* A single type of progenitor cell maintains normal epidermis. *Nature* **446,** 185–189 (2007).
29. Jensen, K. B. *et al.* Lrig1 expression defines a distinct multipotent stem cell population in mammalian epidermis. *Cell Stem Cell* **4,** 427–439 (2009).
30. Soriano, P. Generalized lacZ expression with the ROSA26 Cre reporter strain. *Nature Genet.* **21,** 70–71 (1999).
31. Vasioukhin, V., Degenstein, L., Wise, B. & Fuchs, E. The magical touch: genome targeting in epidermal stem cells induced by tamoxifen application to mouse skin. *Proc. Natl Acad. Sci. USA* **96,** 8551–8556 (1999).
32. Crowson, A. N. Basal cell carcinoma: biology, morphology and clinical implications. *Mod. Pathol.* **19 Suppl 2,** S127–S147 (2006).
33. Harfe, B. D. *et al.* Evidence for an expansion-based temporal Shh gradient in specifying vertebrate digit identities. *Cell* **118,** 517–528 (2004).
34. St-Jacques, B. *et al.* Sonic hedgehog signaling is essential for hair development. *Curr. Biol.* **8,** 1058–1068 (1998).
35. Means, A. L., Xu, Y., Zhao, A., Ray, K. C. & Gu, G. A CK19(CreERT) knockin mouse line allows for conditional DNA recombination in epithelial cells in multiple endodermal organs. *Genesis* **46,** 318–323 (2008).
36. Potten, C. S. The epidermal proliferative unit: the possible role of the central basal cell. *Cell Tissue Kinet.* **7,** 77–88 (1974).
37. Ro, S. & Rannala, B. Evidence from the stop-EGFP mouse supports a niche-sharing model of epidermal proliferative units. *Exp. Dermatol.* **14,** 838–843 (2005).
38. Campbell, C., Quinn, A. G., Angus, B., Farr, P. M. & Rees, J. L. Wavelength specific patterns of p53 induction in human skin following exposure to UV radiation. *Cancer Res.* **53,** 2697–2699 (1993).

DOI: 10.1038/ncb2031

METHODS

Mice. K14-CRE[39] and K14-CREER transgenic mice[40] were provided by Elaine Fuchs (The Rockeffeler University, NY). Shh-CREER knock-in mice[41], K15-CREPR[42] transgenic mice, *RosaSmoM2* mice[43], *Rosa–YFP* and *Rosa–LacZ*[44] mice were obtained from Jackson Laboratory. The K19-CREER knock-in mice[45] were provided by Guoqiang Gu (The Vanderbilt University Medical Center). K14-CREER, Shh-CREER, K15-CREPR and K14-CRE were mated with *RosaSmoM2* and *RosaYFP* mice. Mouse colonies were maintained in a certified animal facility in accordance with European guidelines. At least 50 *RosaSmoM2* mice have been analysed for each CREER line used in this study. For each time-point, at least two mice from two different litters were used to characterize the different phenotype.

Generation of K15-CREER mice. The CREERT2 fragment was amplified from the vector pCre-ERT2[46] (provided by P.Chambon, IGBMC, Illkirch, France) and the K15 promoter fragment[47] was amplified using published primers. The two fragments were cloned in a pBSIISK plasmid. The resulting K15-CREERT2 fragment was microinjected into fertilized oocytes (performed by the UCL facility (P. Jacquemin Laboratory, Université Catholique de Louvain, Belgium)). Transgenic founders were first identified by PCR. Expression profiles of the founders were screened with reporter *RosaYFP* mice. The transgenic founder number 12, which targeted more specifically the bulge cells, was then crossed with *RosaSmoM2*.

Targeting oncogene activation. For non-clonal induction, K14-CREER/*RosaSmoM2* mice were treated with tamoxifen (15 mg, diluted in sunflower oil; Sigma-Aldrich) by intraperitoneal injection in mice aged 23–28 day. Shh-CREER/*RosaSmoM2* mice were induced with tamoxifen (25 mg, diluted in ethanol) by topical application from day 25 (D25) to D30. K15-CREPR/*RosaSmoM2* mice were topically induced with RU486 (2.5 mg/day, diluted in ethanol; Sigma-Aldrich) from D21–D23. K15-CREER/*RosaSmoM2* mice were induced with tamoxifen (2 mg/day), administered intraperitoneally, from D21–D23. K19-CREER/*RosaSmoM2* mice were induced with tamoxifen (2.5 mg/day), administered intraperitoneally, from D28–D32. K14-CREER and Shh-CREER mice were killed 1 week after induction, and the K15-CREPR mice were killed 2 days after induction as induction control and at different time-points to determine which mice developed tumours.

Clonal induction. K14-CREER/*RosaSmoM2* were treated at D28 with tamoxifen (1 mg) and mice were killed every week until 15 weeks after induction. Shh-CREER/*RosaSmoM2* mice were treated at D28 with tamoxifen (1mg). For morphogenesis, Shh-CREER/*RosaSmoM2* mice were treated with tamoxifen (0.2 mg) on postnatal day 1 and killed 1, 6 and 10 weeks after induction.

Macroscopic pictures. Pictures were taken 10 weeks after tamoxifen administration using the Leica MZ16F microscope and the software Leica Application Suite (Leica Microsystems GmbH).

Histology, immunostaining and imaging. Tissues from *RosaSmoM2* mice were processed in OCT and sections were fixed in 4% PAF for 10 min at room temperature, whereas tissues from *Rosa–YFP* mice were pre-fixed for 2h in 4% PAF and processed in OCT. Samples were cut in 5–8 µm sections using CM3050S Leica cryostat (Leica Microsystems GmbH). Because of the presence of IRES YFP following *RosaSmoM2* constructs, *SmoM2*-expressing cells were detected using an anti-GFP antibody.

The following primary antibodies were used: anti-K14 (rabbit, 1:2000, Covance), anti-GFP (rabbit, 1:1000, Molecular Probes), anti-GFP (chicken, 1:4000, Abcam), anti-GFP (goat, 1:2000, Abcam), anti-β4 (rat, 1:200, BD), anti-KI67 (rabbit, 1:200, Abcam), anti-K17 (rabbit, 1:6000, provided Pierre Coulombe, John Hopkins University, MD), anti-K15 (chicken, 1:15000, Covance), anti-P-Cadh (rat, 1:200, Invitrogen), anti-K10 (rabbit, 1:2000, Covance), anti-Gli2 (rabbit, 1/2000, Abcam), anti-CD34 (rat, 1/100, BD), anti-MTS24 (rat, 1/100, provided by Richard Boyd, Monash Immunology and Stem Cell Laboratory, Monash University, Victoria, Australia). Sections were incubated in blocking buffer (PBS/NDS 5%/ BSA 1%/Triton 0.2%) for 1 h at room temperature. Primary antibodies were incubated overnight at 4°C. Sections were rinsed three times in PBS and incubated with secondary antibodies diluted at 1:400 for 1 h at room temperature. The following secondary antibodies were used: anti-rabbit, anti-rat, anti-chicken, anti-goat conjugated to AlexaFluor488 (Molecular Probes), to rhodamine Red-X (JacksonImmunoResearch) or to Cy5 (Jackson ImmunoResearch). Nuclei were stained in Hoechst solution and slides were mounted in DAKO mounting medium supplemented with 2,5% Dabco (Sigma).

For mouse mononoclonal antibodies AE13 (mouse, 1:100, Abcam) and AE15 (mouse, 1:100, Abcam), immunostainings were performed following MOM kit instructions. Sections were incubated in MOM blocking with 10 µg ml^{-1} anti-mouse Fab (Jackson Immunoresearch) for 1 h. Incubation of primary antibodies was performed in MOM diluent solution overnight at 4°C. Slides were then washed and incubated with secondary antibodies as described above.

Pictures were acquired using the Axio Imager M1 Microscope, the AxioCamMR3 or MrC5 camera and using the Axiovision software (Carl Zeiss Inc.).

Haematoxylin and eosin staining protocol. Haematoxilin (Mayer) staining was performed for 4 min followed by serial wash immersion in distilled water, 5 min in tap water, 10 quick washes in 70% ethanol: 0.1% HCl and finally in distilled water. Eosin staining was performed for 20 s and washed in tap water. Sections were dehydrated by serial immersions of 1 min each in 70%, 80%, 85%, 90%, 95%, and 100% ethanol, followed by two washes for 10 min in 100% Toluol. Slides were mounted in safe mount (Sigma).

Confocal microscopy analysis of whole mount tail epidermis. Tail skin from K14-CREER/*RosaSmoM2* or Shh-CREER/*RosaSmoM2* were incubated 4 h in EDTA 5 mM at 37°C and dermis and epidermis were separated as described previously[48]. The epidermis was fixed 2 h in PAF 4% at room temperature and washed 3 times for 10 min in PBS. Tail epidermis was blocked 4 h in PBS/BSA 1%/NDS 5%/triton 0.75% and incubated in rocking-plate overnight at room temperature with anti-GFP (rabbit, 1:500; Molecular Probes) and anti-β4 (rat, 1:50; BD). After 3 washes of 1 h, the tail epidermis was incubated overnight at room temperature with anti-rabbit conjugated to Alexa488 (1:300), anti-rat conjugated to RRX (1:400). Nuclei were stained by ToPro-3 iodide (1/500) (invitrogen). Pictures were acquired using the Zeiss LSM510 Meta Microscope and using the LSM510 software (Carl Zeiss).

Isolation of keratinocytes and RNAs extraction. Isolation of keratinocytes was performed as described previously[49]. Briefly, Tail skins from K14-CREER/*RosaSmoM2* at 4 weeks after induction, from K19-CREER/*RosaSmo* at 8 weeks after induction and from wild-type mice were cleaned from adipose tissue and blood vessels and incubated overnight in trypsin/EDTA at 4°C (Gibco-invitrogen). After isolation of keratinocytes, immunostaining was performed using Alexa647-conjugated anti-CD34 (clone RAM34; BD Biosciences) and PE-conjugated anti-α6-integrin (clone GoH3; BD biosciences) as described previously[49]. Living epidermal cells expressing *SmoM2* were gated by forward scatter, side scatter and by negative staining for Hoechst and by expression of YFP. Fluorescence-activated cell sorting analysis was performed using FACSAria and FACSDiva software (BD Biosciences). Sorted cells were collected directly in the lysis buffer provided by the manufacturer (Microprep kit, RNAeasy, Stratagen) and RNA extraction was performed according to the manufacturer's protocol. The entire procedure was repeated in four biologically independent samples.

Reverse transcription and quantitative PCR (qPCR). Total RNA extraction and DNase treatment of samples were performed using the microprep kit (Stratagen) according to the manufacturer's recommendations. After nanodrop quantification, purified RNA was used to synthesize the first strand cDNA in a 50 µl final volume, using a SuperscriptII (Invitrogen) and random hexamers (Roche). Control of genomic contaminations was measured for each sample by performing the same procedure with or without reverse transcriptase. qPCR analysis were performed with 2 ng of cDNA reaction as template, except for Gli2 analysis in which 5 ng of cDNA reaction, using a Brilliant II Fast SYBR QPCR Master Green mix (Stratagen) an a Agilent technologies stratagene Mx3500P real-time PCR system. Relative quantitative RNA was normalized using the housekeeping genes β-actin and HPRT. Primers were designed using Lasergene 7.2 software (DNAStar Inc) and are presented below. Analysis of the results was performed using Mxpro software (Stratagene). The entire procedure was repeated in three biologically independent samples. Error bars represent standard error of the mean (s.e.m.). Results were presented as the fold changes over wild-type cells isolated from the same epidermal compartments.

Quantification of the number of clones induced per pilosebaceous unit. A minimum of 110 pilosebaceous units from three separate mice were studied per condition for K14CREER/*RosaSmoM2* mice. For each unit, the number of YFP-expressing clones was counted in each compartment (interfollicular epidermis, infundibulum, bulge, sebaceous and lower follicle). The mean number of clones for each compartment at the different time-points studied was then normalized as the percentage of the mean number of clones counted one week post induction. Error bars represent s.e.m.

Distribution of hair follicle histology. 50 pilosebaceous units (from two different mice) were studied per condition for K15CREPR/*RosaSmoM2* mice at each time-point. A minimum of 125 pilosebaceous units in two different mice was studied per condition for K19CREER/*RosaSmoM2* mice. Each follicle was counted as negative if no *SmoM2*-expressing cells were detected, or classified as normal, hyperplastic (increase number of cells with normal morphology), dysplastic (cells with abnormal morphology) or BCC-positive, and the distribution of the different histological phenotypes was plotted as the percentage of the total number of follicles studied.

For ShhCREER/*RosaSmoM2* induced at D1, a total of 1,380 pilosebaceous units from two different mice were studied at 10 weeks post induction. Each follicle was counted as negative if no *SmoM2*-expressing cells were detected, or classified as normal, hyperplastic, dysplastic or BCC positive, and the results presented as a table.

Quantification of SmoM2-expressing clones in Shh-CREER/RosaSmoM2 mice. Mice were induced with tamoxifen (0.2 mg) at birth (D1). Mice were sacrified 1 week after induction. Quantification of *SmoM2*-expressing clones showed that 76% of the pilosebaceous units were labelled one week after tamoxifen administration (570 SmoM2 hair follicle clones in 753 hair follicles analysed) and 3% of the infundibulum contained SmoM2 clones (24 *SmoM2* infundibulum clones in 753 hair follicles analysed). Whereas, only 10% of hair follicles contained *SmoM2*-expressing clones 10 weeks after tamoxifen administration (137 out of 1380 hair follicles), the number of SmoM2 clones within the infundibulum remained stable (2.5% of infundibulum).

List of the primers used for the real-time PCR analysis. Ptch1 F: TGGCTGGCGTCCTGTTGGTTG; Ptch1 R: ACGCTCGCAGGGCAGGGATAG; Ptch2 F: CCCCACCTGACACCCCTCTCC; Ptch2 R: ATGCCCACTGGTACTGCTCTGTCC; Gli1 F: GTCCGCGCCTCTCCCACATACTA; Gli1 R: CATAACCCTGGGACCCTGACATAA; Gli2 F: ACGCGCCTTTGCCGATTGAC; Gli2 R: CTGGGGCTGCGAGGCTAAAGAG;

39. Vasioukhin, V., Bauer, C., Degenstein, L., Wise, B. & Fuchs, E. Hyperproliferation and defects in epithelial polarity upon conditional ablation of α-catenin in skin. *Cell* **104,** 605–17 (2001).
40. Vasioukhin, V., Degenstein, L., Wise, B. & Fuchs, E. The magical touch: genome targeting in epidermal stem cells induced by tamoxifen application to mouse skin. *Proc. Natl Acad. Sci. USA* **96,** 8551–6 (1999).
41. Harfe, B. D. *et al.* Evidence for an expansion-based temporal Shh gradient in specifying vertebrate digit identities. *Cell* **118,** 517–28 (2004).
42. Morris, R. J. *et al.* Capturing and profiling adult hair follicle stem cells. *Nature Biotechnol.* **22,** 411–7 (2004).
43. Mao, J. *et al.* A novel somatic mouse model to survey tumorigenic potential applied to the Hedgehog pathway. *Cancer Res.* **66,** 10171–8 (2006).
44. Soriano, P. Generalized lacZ expression with the *ROSA26* Cre reporter strain. *Nature Genet.* **21,** 70–1 (1999).
45. Means, A. L., Xu, Y., Zhao, A., Ray, K. C. & Gu, G. A CK19(CreERT) knock-in mouse line allows for conditional DNA recombination in epithelial cells in multiple endodermal organs. *Genesis* **46,** 318–23 (2008).
46. Indra, A. K. *et al.* Temporally-controlled site-specific mutagenesis in the basal layer of the epidermis: comparison of the recombinase activity of the tamoxifen-inducible Cre-ER(T) and Cre-ER(T2) recombinases. *Nucleic Acids Res.* **27,** 4324–7 (1999).
47. Liu, Y., Lyle, S., Yang, Z. & Cotsarelis, G. Keratin 15 promoter targets putative epithelial stem cells in the hair follicle bulge. *J. Invest. Dermatol.* **121,** 963–8 (2003).
48. Braun, K. M. *et al.* Manipulation of stem cell proliferation and lineage commitment: visualisation of label-retaining cells in whole-mounts of mouse epidermis. *Development* **130,** 5241–55 (2003).
49. Blanpain, C., Lowry, W. E., Geoghegan, A., Polak, L. & Fuchs, E. Self-renewal, multipotency, and the existence of two cell populations within an epithelial stem cell niche. *Cell* **118,** 635–48 (2004).

nature cell biology

DOI: 10.1038/ncb2031

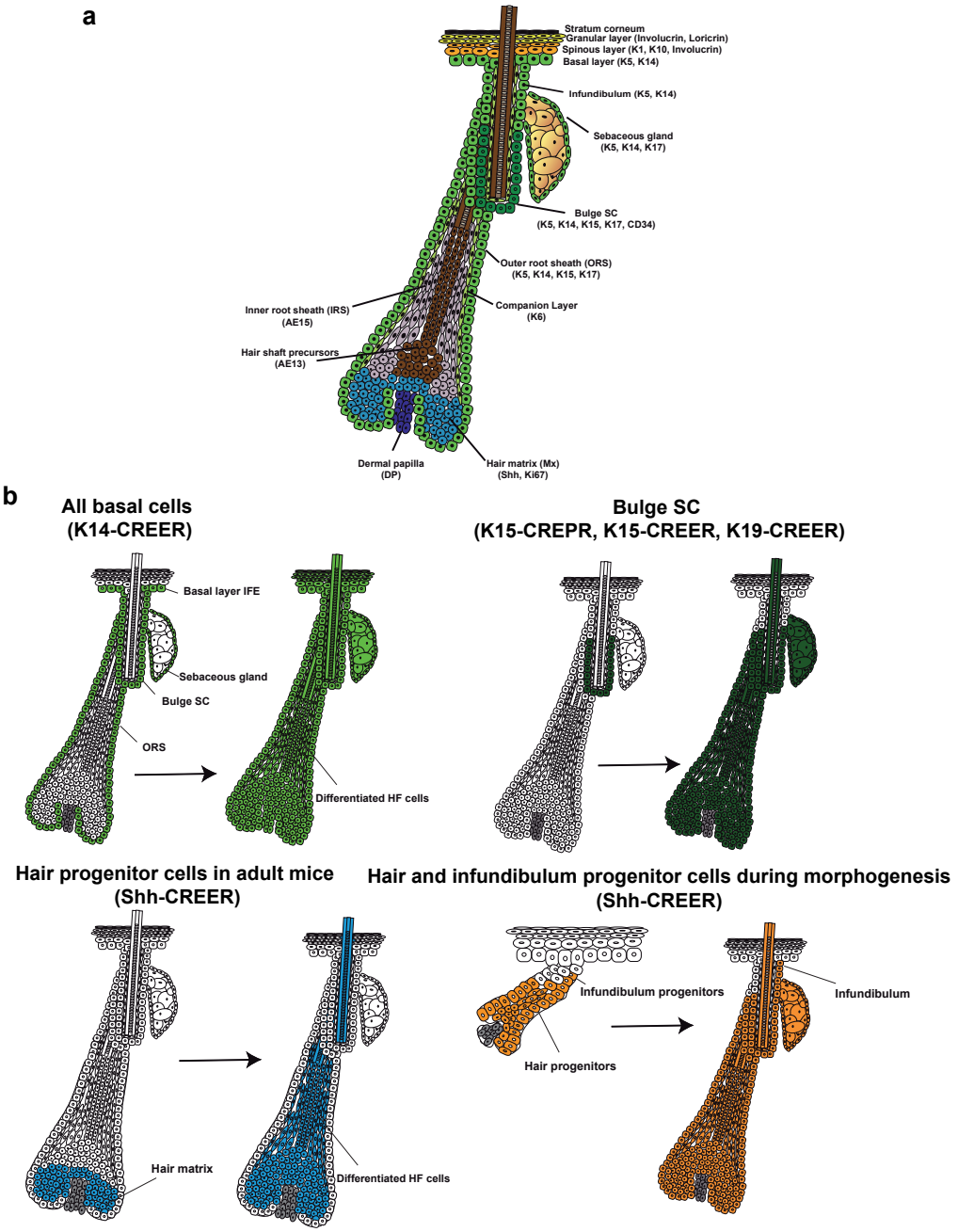

Figure S1 Organization of the pilosebaceous unit and the inducible CRE mice used to target the different epidermal compartments. (**a**) Cartoon depicting the organization of the pilosebaceous unit in the epidermis. Specific markers for each epidermal compartment are put in brackets. (**b**) Summary of the different inducible CRE mice used in this study and the epidermal lineages targeted following CRE activation. Epidermal compartments in which CREER is expressed (left) and the cells progenies arising from these compartments (right).

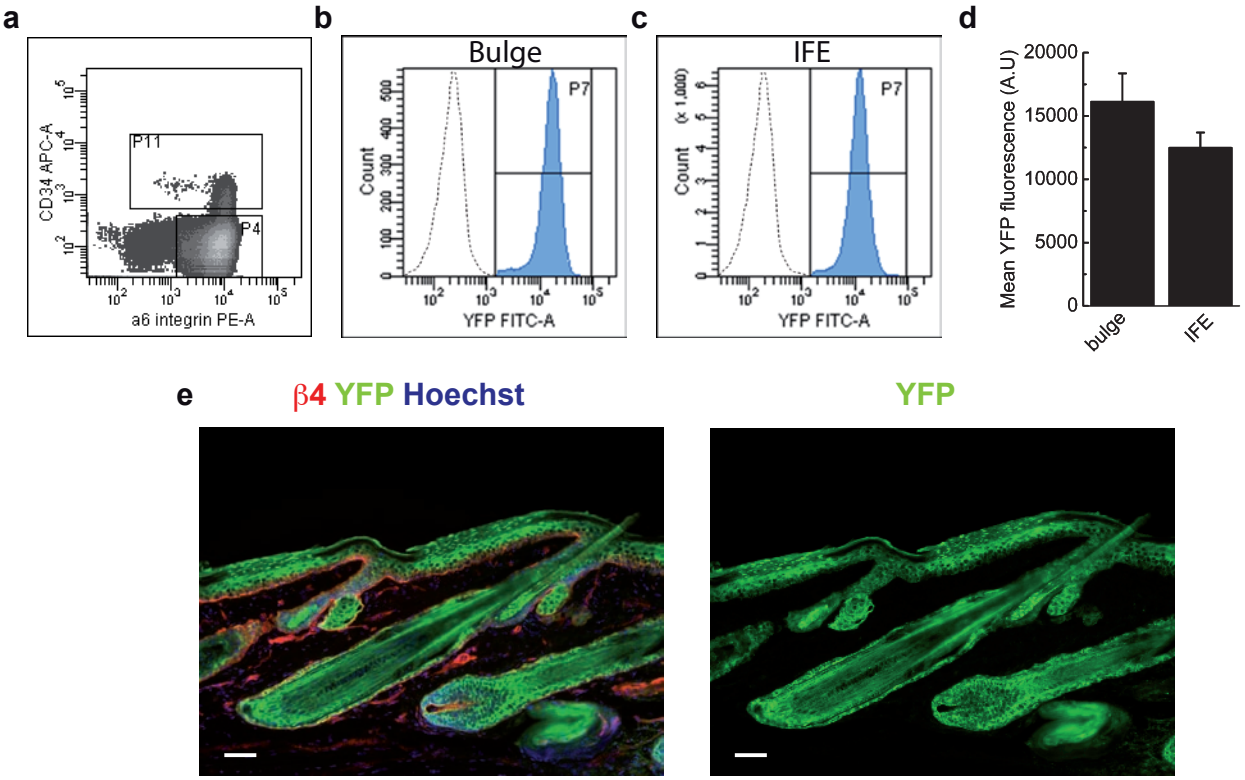

Figure S2 Rosa26 promoter induced expression is equivalent in different compartments of tail epidermis. (**a**) Dot plot of YFP+ cells from K14-CRE/RosaYFP tail epidermal cells stained with α6-integrin Ab (PE) and CD34 Ab (Alexa647). Fluorescence histogram of gated bulge (α6-integrin+/CD34+) (**b**) and gated IFE cells (α6-integrin+/CD34-) (**c**) from K14CRE/RosaYFP mice (filled area). (**d**) Histogram summarizing the mean YFP fluorescence (A.U) from bulge and IFE epidermal cells. (**e**) immunostaining of YFP in the tail epidermis from K14-CRE/RosaYFP mice. Scale bars, 50μm.

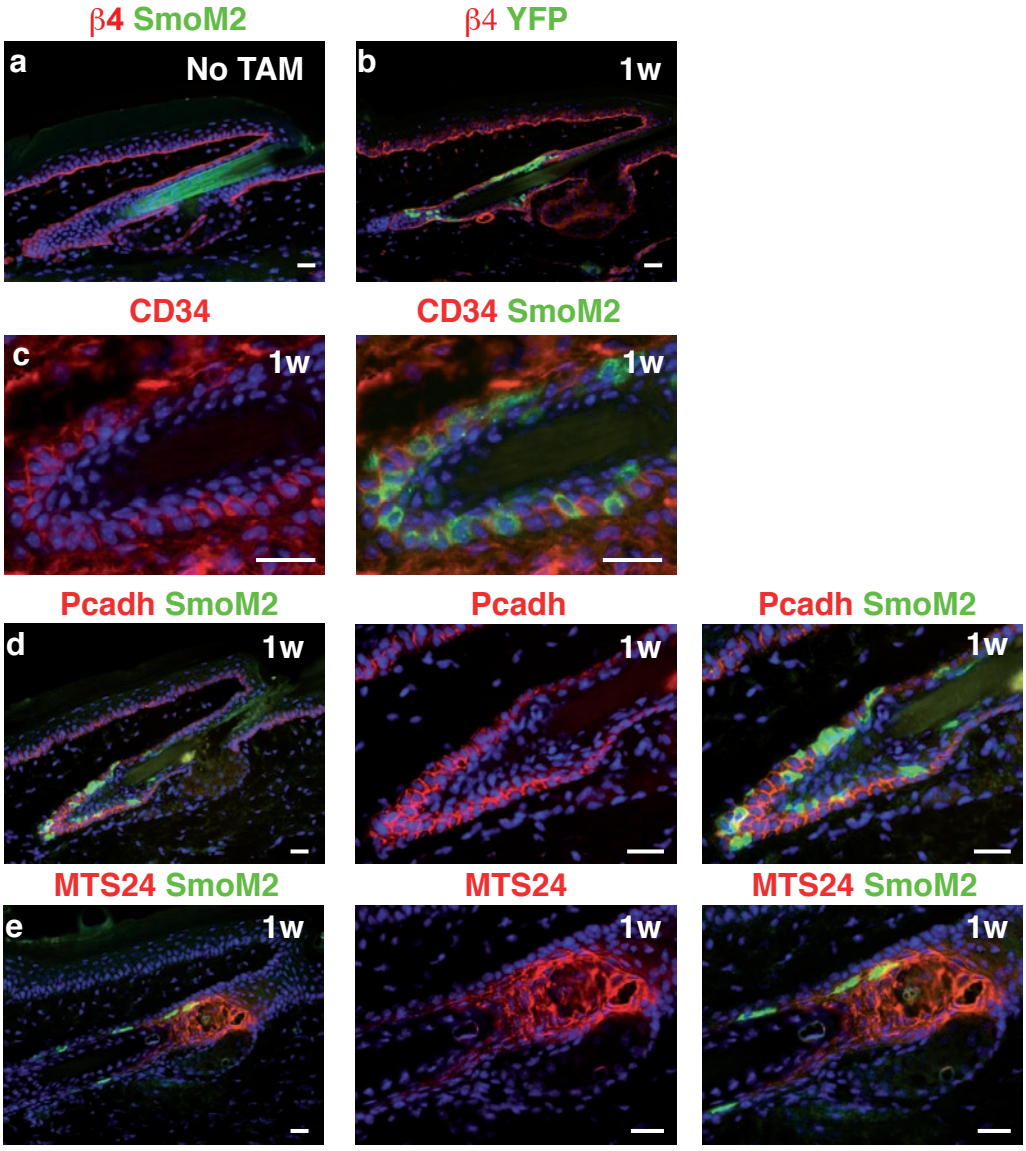

Figure S3 Lineage tracing using K19CREER mice target bulge stem cells and their HF progenies. (**a**) No leakiness in the K19-CREER/RosaSmoM2 mice in absence of tamoxifen. (**b**) Expression of YFP in bulge stem cells and their progenies 1 week following 10 mg tamoxifen induction in K19-CREER/RosaYFP mice. No YFP positive cell is seen above the sebaceous gland (infundibulum and IFE) in these mice at any time following induction. (**c**) CD34 positive cells (bulge stem cells) are targeted in K19-CREER/RosaSmoM2 mice. (**d**) Pcadherin positive cells (ORS cells) are targeted in K19-CREER/RosaSmoM2 mice. (**e**) MTS24 positive cells (isthmus cells) are targeted in K19-CREER/RosaSmoM2 mice. Scale bars, 50 μm.

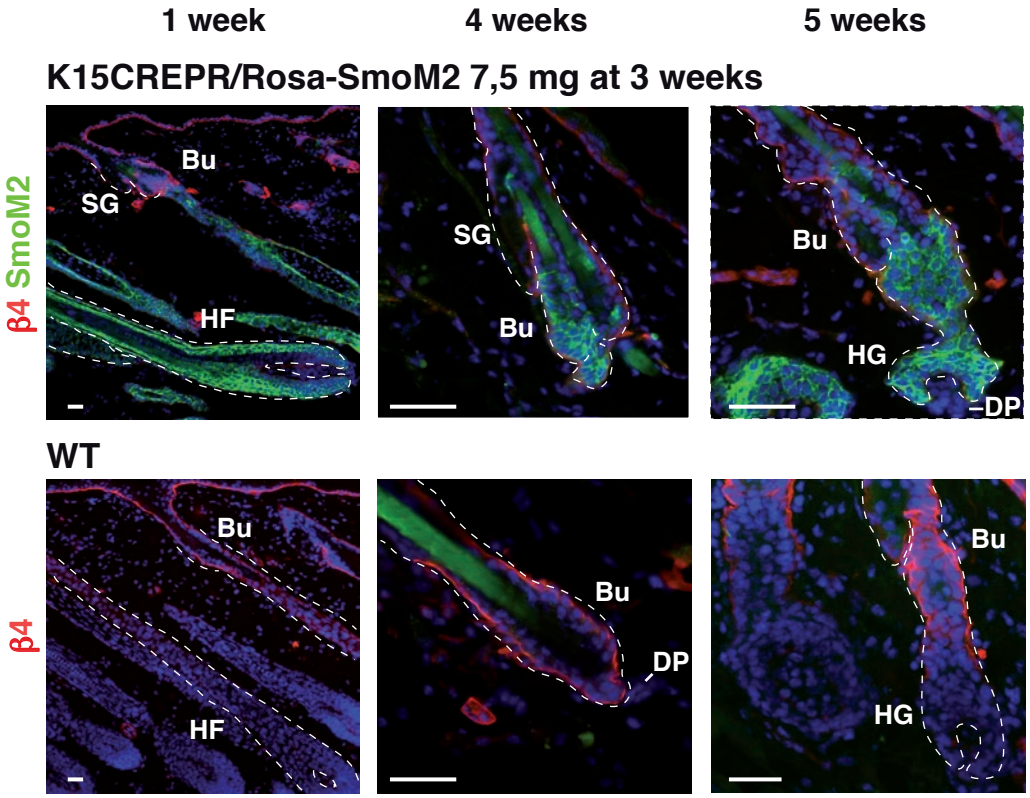

Figure S4 Hair cycle is normal in mice expressing SmoM2 in HF. SmoM2 targeted cells in backskin 1 week, 4 weeks and 5 weeks following induction. Lower panels show WT backskin at the same age. Bu, Bulge; DP, Dermal Papilla; HF, Hair follicle; HG, Hair germ; SG, Sebaceous Gland. Scale bars, 50 μm.

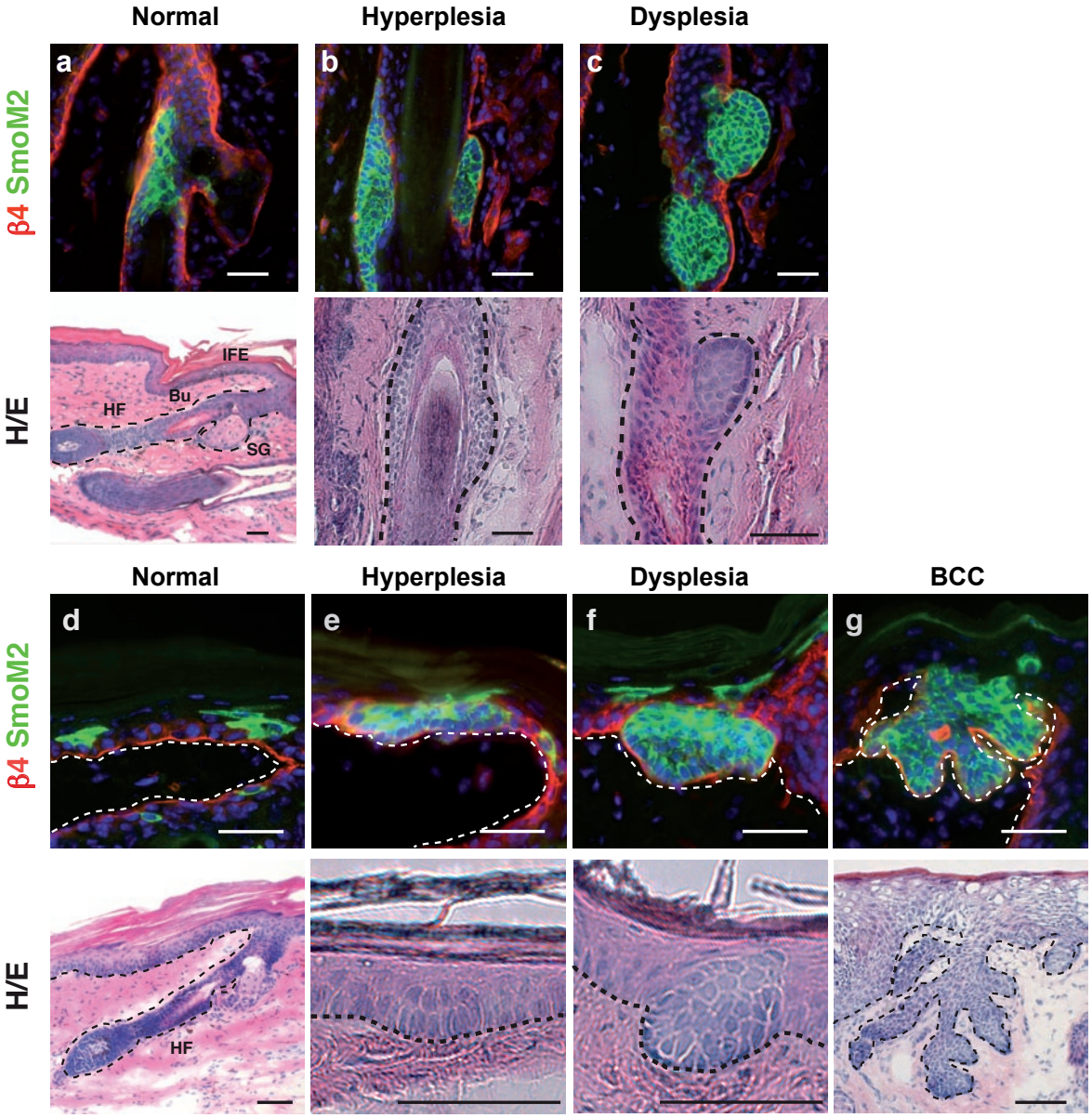

Figure S5 Histology of SmoM2 expressing cells in HFs and in the interfollicular tail epidermis. Examples of normal (**a**), hyperplastic (**b**) and dysplastic (**c**) morphology in hair follicle of K15CREPR/RosaSmoM2 mice following 7,5 mg RU486. Examples of normal (**d**), hyperplastic (**e**), dysplastic (**f**) and BCC (**g**) clones in tail interfollicular epidermis of K14-CREER/RosaSmoM2 mice following 1mg tamoxifen administration. Immunofluorescence, βb4-integrin/SmoM2. H/E, haematoxylin eosin staining. Scale bars, 50 μm.

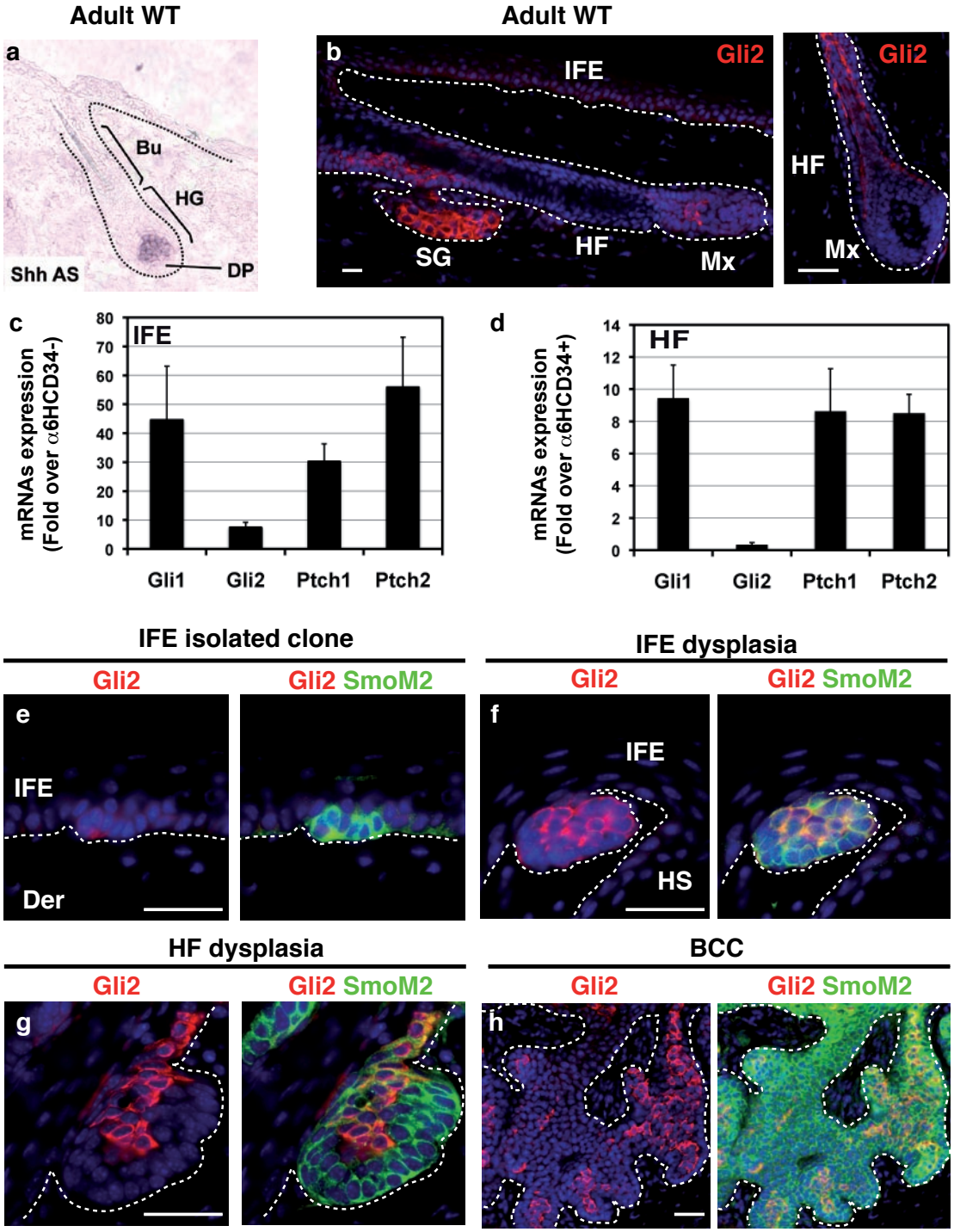

Figure S6 Expression of Gli2 following SmoM2 expression. (**a**) In situ hybridization of Shh in adult WT backskin. (**b**) Expression of Gli2 in adult WT tail. (**c**,**d**) Real time RT-PCR performed on sorted IFE and bulge stem cells 4 weeks following TAM administration in K14-CREER (**c**) and K19-CREER mice (**d**). (**e**-**h**), Expression of Gli2 in isolated SmoM2 clone in K14-CREER/RosaSmoM2 1 week after induction (**e**), in IFE (**f**) and HF (**g**) dysplastic and in BCC (**h**) lesions. Der, Dermis; HF, Hair Follicle; HS, Hair Shaft; IFE, Interfollicular epidermis; Mx, Matrix; SG, sebaceous Gland. Scale bars, 25 μm. Error bars, 1 s.e.m. Slides were mounted in safe mount (Sigma).